International Journal of Nanomedicine

Dovepress
Taylor & Francis Group

Open Access Full Text Article

ORIGINAL RESEARCH

Chitosan-Coated PLGA Nanoparticles for Sustained Delivery of Epigallocatechin Gallate and Differential Cytotoxicity in HepG2 and HepaRG Cells

Sharareh Shahroudi, Erfan Salahinejad

Faculty of Materials Science and Engineering, K. N. Toosi University of Technology, Tehran, Iran

Correspondence: Erfan Salahinejad, Email salahinejad@kntu.ac.ir

International Journal of Nanomedicine downloaded from https://www.dovepress.com/
For personal use only.

Introduction: Epigallocatechin-3-gallate (EGCG) is a green-tea catechin with well-documented antiproliferative activity, but its short half-life and poor stability in physiological media limit its application. This study aimed to develop chitosan-coated poly(lactic-co-glycolic acid) (PLGA) core-shell nanoparticle carriers for EGCG, with assessing the effect of the chitosan shell on their release kinetics and concentration-response behavior in hepatic carcinoma and non-tumorigenic hepatic cells in vitro.

Methods: EGCG-loaded PLGA nanoparticles were prepared by emulsion solvent evaporation at nominal loadings of 0.5, 1, and 1.5 wt% and then coated with chitosan. Morphology and size were characterized by field-emission scanning electron microscopy (FE-SEM), chemical composition by Fourier-transform infrared spectroscopy (FTIR), and EGCG release in phosphate-buffered saline (PBS) up to 30 days by UV-Vis spectroscopy. Release profiles were fitted to the zero-order, first-order, Higuchi and Korsmeyer-Peppas models. Metabolic cell viability was assessed by MTT assay in human hepatocellular carcinoma HepG2 cells and non-tumorigenic hepatic HepaRG cells until 5 days, and the concentration-response data were fitted with a Hill model.

Results: The uncoated and chitosan-coated particles had mean diameters of 117 ± 8 and 144 ± 6 nm, respectively, giving an estimated dry shell thickness of 13.5 ± 5.0 nm. The application of the chitosan shell reduced the first 24 h burst release from 25.7 to 10.3–15.6% and extended the profile to a plateau from 25 to 27 days. Release from the coated formulations was best described by the Higuchi model, with Korsmeyer-Peppas exponents of 0.55–0.63 indicating anomalous (non-Fickian) transport, against n = 0.46 showing Fickian transport for the uncoated reference. Encapsulation efficiencies were 85.2–88.8%, corresponding to delivered EGCG doses of 4.26–12.98 μg mL^{-1} at the applied nanoparticle concentration of 1 mg mL^{-1}. HepG2 metabolic viability decreased in a concentration-dependent manner to 26.4 ± 1.8% of the untreated control on day 5, corresponding to 73.6% growth inhibition, with a fitted IC_{50} of 8.2 μg mL^{-1}. Over the same dose range, HepaRG viability remained at or above 92.4% and no IC_{50} was reached (>13 μg mL^{-1}). The drug-free carrier was non-cytotoxic in both cell lines.

Conclusion: A chitosan shell on EGCG-loaded PLGA nanoparticles suppresses burst release and shifts the transport mechanism from Fickian to anomalous, producing sustained release to 27 days. The resulting formulations reduce HepG2 metabolic viability in a concentration-dependent manner, while leaving HepaRG viability above the ISO 10993–5 cytotoxicity threshold.

Keywords: natural anticancer compounds, drug delivery, release kinetics, nanocarriers

Introduction

Cancer is one of the leading causes of mortality worldwide. Conventional cancer treatments include surgery, hormone therapy, radiotherapy, and chemotherapy. However, these therapeutic approaches suffer from several limitations, including high cost, short half-life of therapeutic compounds, poor solubility of chemotherapeutic drugs, severe toxicity, and numerous side effects.[1,2] Natural compounds have emerged as promising alternatives for cancer treatment owing to high biological performance, low cost, and slight side effects. Among them, epigallocatechin-3-gallate (EGCG), the main health-related ingredient in green tea, has attracted considerable attention for cancer therapy applications. The anticancer

https://doi.org/10.2147/IJN.S647028
Received: 13 August 2026
Accepted: 27 October 2026
Published: 2 November 2026

© 2026 Shahroudi and Salahinejad. This work is published and licensed by Dove Medical Press Limited. The full terms of this license are available at https://www.dovepress.com/terms.php and incorporate the Creative Commons Attribution – Non Commercial (unported, v4.0) License (http://creativecommons.org/licenses/by-nc/4.0/). By accessing the work you hereby accept the Terms. Non-commercial uses of the work are permitted without any further permission from Dove Medical Press Limited, provided the work is properly attributed. For permission for commercial use of this work, please see paragraphs 4.2 and 5 of our Terms (https://www.dovepress.com/terms.php).

activity of EGCG has been indicated in both in-vitro[3,4] and in-vivo[5,6] studies, as supported by clinical investigations in humans.[7] Despite its high therapeutic potential, EGCG suffers from poor stability and a short half-life, limiting its clinical application.[8,9] Therefore, strategies capable of improving EGCG stability while maintaining a therapeutically useful local concentration are highly required.

Polymeric nanocarrier-based drug delivery systems provide an effective approach for improving the delivery behavior of anticancer agents.[8,10] These nanoparticles are capable of encapsulating therapeutic agents and can serve as carriers for targeted drug delivery through surface modification or encapsulation strategies. Surface engineering of a nanocarrier can integrate several functions within a single architecture, including the protection of the payload, modulation of its release rate and responsiveness to the local environment, which is the design principle underlying core-shell carriers. Several polymeric nanocarrier-based systems have been investigated to improve the delivery and anticancer efficacy of EGCG. Minnelli et al[11] developed EGCG-loaded poly(lactic-co-glycolic acid (PLGA) nanoparticles for lung cancer therapy, but lacked an active tumor-targeting ligand and therefore relied mainly on passive accumulation. In another study, Kazi et al[12] designed folate peptide-decorated EGCG-loaded PLGA nanoparticles for folate receptor-positive breast cancer cells, including MDA-MB-231 and MCF-7 cells. Although folate decoration improved cellular targeting, the relatively lower encapsulation efficiency compared with non-targeted PLGA-EGCG nanoparticles and the absence of a fully stimuli-responsive release mechanism limited its ability to provide both high drug payload and precise intracellular release. Similarly, PEGylated EGCG-loaded PLGA-based nanoparticles have been reported, showing that PEGylation can improve colloidal stability and prolong EGCG release. Nevertheless, PEGylation mainly contributes to steric stabilization and immune evasion, while it does not necessarily ensure strong cellular adhesion or receptor-mediated tumor localization.[13]

To our knowledge, no EGCG delivery system has yet been reported to simultaneously provide high encapsulation efficiency, protection against premature degradation, and sustained release with a strongly suppressed initial burst. We hypothesize that constructing a chitosan-coated PLGA core–shell nanoparticle system for EGCG delivery will (i) significantly reduce the initial burst release observed in conventional PLGA–EGCG formulations and prolong the release period, and (ii) yield a concentration-dependent reduction of metabolic viability in hepatic carcinoma cells over a dose range, with leaving non-tumorigenic hepatic cells above the accepted cytotoxicity threshold. This dual functionality is expected to arise from the complementary roles of the nanoparticle components: the PLGA core provides high encapsulation efficiency and protection against premature drug degradation, although it is associated with an undesirable initial burst release and limited tumor-targeting capability.[14,15] In contrast, the chitosan shell acts as an additional diffusion barrier that regulates the burst release and extends the release period.[16]

Materials and Methods

Materials

PLGA (lactic acid: glycolic acid ratio of 50:50, molecular weight: 17,000), chitosan (degree of deacetylation: 84.2%, weight-average molecular weight (M_w): 140 kDa), polyvinyl alcohol (PVA, fully hydrolyzed, molecular weight: 130,000), and epigallocatechin-3-gallate (EGCG, purity > 98%) were provided from Sigma-Aldrich. Phosphate-buffered saline (PBS, pH: 7.4), chloroform ($CHCl_3$), and glacial acetic acid (CH_3COOH) were obtained from Merck. 3-(4,5-Dimethylthiazol-2-yl)-2,5-diphenyltetrazolium bromide (MTT), fetal bovine serum (FBS), L-glutamine, dimethyl sulfoxide (DMSO), streptomycin, penicillin, and trypsin-EDTA solution were also purchased from Sigma-Aldrich.

Fabrication of EGCG-Loaded PLGA Nanoparticles

EGCG-loaded PLGA nanoparticles were fabricated using an emulsion solvent evaporation method, according to a previously reported procedure.[17] Briefly, 5 mL of 1 wt% PLGA solution in chloroform was prepared under magnetic stirring for 2 h. 0.5, 1, and 1.5 wt% EGCG relative to the dry weight of PLGA were added to 0.5 mL PBS. The PLGA solution was then added to the PBS solution and sonicated for 2 min at a frequency of 4 Hz to form the primary water-in-oil (W1/O) emulsion. To prepare the secondary aqueous phase, PVA was dissolved in water under magnetic stirring for 24 h to obtain 10 mL of 1 wt% PVA solution (W2). The W1/O emulsion was subsequently added to the W2 phase and

emulsified for 1 min at a frequency of 8 Hz. The resulting emulsion was magnetically stirred for 24 h to allow the complete evaporation of chloroform. Nanoparticles were then collected by centrifugation at 4000 rpm for 20 min and washed twice with distilled water through centrifugation. Finally, the prepared nanoparticles were frozen and dried using a freeze dryer at −60 °C for 24 h.

Chitosan Coating of EGCG-Loaded PLGA Nanoparticles

The EGCG-loaded PLGA particles were coated with chitosan according to the method reported by Chronopoulou et al.[18] A predetermined amount of the nanoparticles was immersed in a 1 wt/v chitosan solution prepared in acetic acid. The suspension was maintained under magnetic stirring at room temperature for 24 h. Then, the suspension was centrifuged at 4000 rpm and the supernatant was discarded. The remaining precipitate was washed twice with distilled water and recollected by centrifugation. Finally, the nanoparticles were freeze-dried. Table 1 summarizes the specifications of the fabricated samples along with their designations. The schematic illustration of the fabrication process for the EGCG-loaded, chitosan-coated PLGA nanoparticles is presented in Figure 1.

Structural Characterizations

The morphology of the synthesized nanoparticles was evaluated using field-emission scanning electron microscopy (FE-SEM, MIRA3 TESCAN-XMU, Working voltage = 30kV). Particle size was obtained from the FE-SEM micrographs using ImageJ by measuring a minimum of 50 individual particles per sample. Fourier-transform infrared spectroscopy (FTIR) analysis was performed using an AVATAR Thermo spectrometer within the wavenumber range of 4000–400 cm^{-1} and resolution of 1 cm^{-1}.

In-vitro Drug Release Evaluations

The release behavior of EGCG from the fabricated nanoparticles was investigated in-vitro. For this purpose, 1 mg of the nanoparticles was immersed in 1 mL PBS (pH = 7.4) and incubated at 37°C. The concentration of released EGCG at different time points was determined using ultraviolet–visible (UV–Vis) spectroscopy (Aurora, Bloorazma) at a wavelength of 274 nm.[19]

Absorbance readings were blank-corrected against plain PBS. Quantification was based on a calibration curve of EGCG in PBS (pH 7.4), constructed over the range 0.1–20 µg/mL using 8 concentration levels. The limits of detection and quantification were calculated as 3.3σ/S and 10σ/S, respectively, using the residual standard deviation of the calibration curve, in accordance with ICH Q2(R1).[20] The equations used to determine the encapsulation efficiency, drug loading content, and released drug level are presented below:

$$\text{Encapsulation Efficiency, EE}(\%) = (\text{Weight of drug encapsulated}/\text{Total initial drug weight}) \times 100 \quad (1)$$

$$\text{Drug Loading Content, DLC}(\text{wt}\%) = (\text{Weight of drug encapsulated}/\text{Total weight of nanoparticles}) \times 100 \quad (2)$$

$$\text{Released Drug Level}(\%) = (\text{Amount of drug released at a specific time}/\text{Total amount of drug loaded}) \times 100 \quad (3)$$

Table 1 Specifications of the Samples Fabricated in This Study

Sample Name	EGCG (wt%)	Oil Solution	W1 Solution	W2 Solution	Coating Solution
PLGA-Chi	0	5 mL of 1 wt% PLGA	0.5 mL of PBS solution	10 mL of 1 wt% PVA	1 wt/v chitosan
PLGA-EGCG	1	5 mL of 1 wt% PLGA	0.5 mL of PBS solution	10 mL of 1 wt% PVA	None
PLGA-Chi-0.5EGCG	0.5	5 mL of 1 wt% PLGA	0.5 mL of PBS solution	10 mL of 1 wt% PVA	1 wt/v chitosan
PLGA-Chi-1EGCG	1	5 mL of 1 wt% PLGA	0.5 mL of PBS solution	10 mL of 1 wt% PVA	1 wt/v chitosan
PLGA-Chi-1.5EGCG	1.5	5 mL of 1 wt% PLGA	0.5 mL of PBS solution	10 mL of 1 wt% PVA	1 wt/v chitosan

https://doi.org/10.2147/IJN.S647028

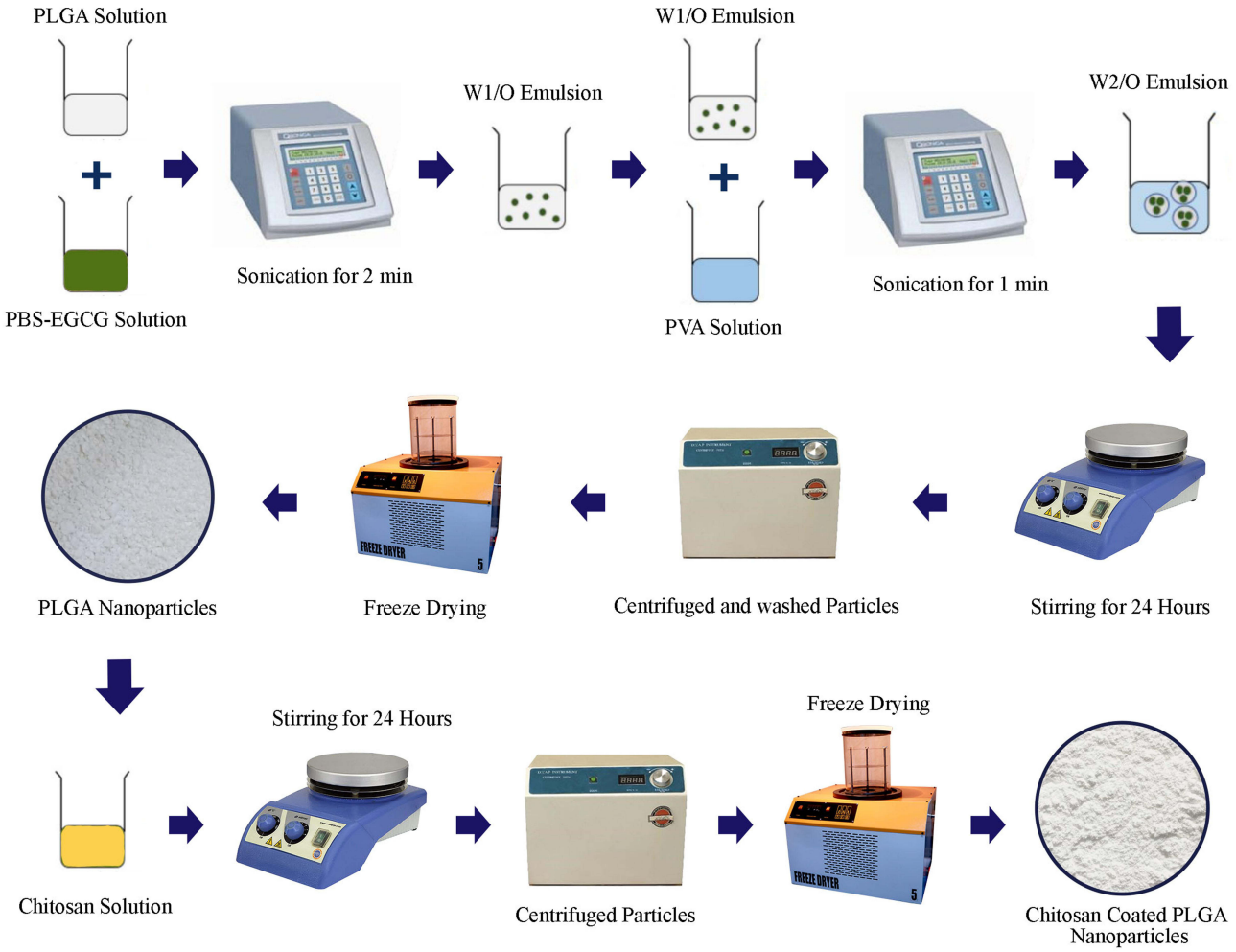


Figure 1 Schematic illustration of the fabrication process of the EGCG-loaded, chitosan-coated PLGA nanoparticles.

The cumulative release profiles were fitted to four kinetic models: zero-order, first-order, Higuchi, and Korsmeyer–Peppas, with the latter model fitted only to the initial 70% of cumulative release. Fitting was performed by nonlinear least squares.

Cellular Metabolic Activity Assays

Metabolic viability was assessed using the MTT colorimetric assay. The human hepatocellular carcinoma HepG2 cell line was obtained from the American Type Culture Collection (ATCC, USA), while the human hepatic HepaRG cell line was obtained from Biopredic International (France). HepG2 is a widely used human liver cancer cell model,[21] whereas HepaRG is a human hepatic cell line capable of differentiation into metabolically competent hepatocyte-like cells and is widely used in drug metabolism and hepatotoxicity studies;[22] Thus, the two cell lines provide complementary models for assessing responses in liver cancer cells and differentiated hepatic cells. Both cell lines are established, commercially available cell lines and were not obtained directly from human participants; therefore, no patient recruitment, informed consent, or patient-derived sample collection was involved in this study. The cells were cultured in RPMI-1640 medium supplemented with 10% (v/v) FBS, 1% (w/v) penicillin–streptomycin, and 1% L-glutamine. All cell cultures were maintained at 37°C in a humidified atmosphere containing 95% humidity and 5% CO_2.

For cell culture, approximately 5×10^5 cells were seeded in 25 cm^2 culture flasks and passaged twice weekly. Cells were detached using trypsin-EDTA solution. The cell suspension was centrifuged at 1000 rpm for 5 min and subsequently resuspended in the culture medium for further experiments. Nanoparticle suspensions in DMSO were prepared

by serial dilution to achieve a final DMSO concentration of [0.1% v/v] in the treatment wells. A vehicle control containing the same DMSO concentration but no nanoparticles was also included to account for potential effects of DMSO. Cultured cells were seeded in well plates at a density of 1×10^4 per well and incubated. The cells were then washed with serum-free medium to minimize the formation of a biomolecular corona and potential binding of released EGCG to serum albumin, which could alter nanoparticle-cell interactions and the free fraction of EGCG.[23,24] The cells were then incubated with the nanoparticle samples at a nanoparticle concentration of 1 mg/mL for 1, 3, and 5 days. Cells cultured only in the serum-free medium were used as the untreated control, serving as the baseline for calculating cell viability. Subsequently, 20 µL of the MTT solution (5 mg/mL) was added to each well and incubation continued for an additional 4 h. The culture medium was then removed and 200 µL DMSO was added to dissolve formed formazan crystals. The optical density was measured at 540 nm using a microplate reader (CLARIOstar, BMG Labtech). Cell viability was calculated according to Equation 4, where *Nt* and *Nc* represent the optical density of the treated and untreated cells, respectively.

$$\text{Cell Viability}(\%) = (N_t/N_c) \times 100 \tag{4}$$

Statistical Analysis

The MTT experiment was performed once, with three technical replicate wells per sample and time point. All values are reported as mean ± standard deviation of these three wells. Comparisons among the groups at each time point were made by one-way analysis of variance (ANOVA) followed by the Tukey honestly significant difference post-hoc test, with a significance threshold of $p < 0.05$, using GraphPad Prism 9.

Concentration-response relationships were obtained by fitting the day-5 data to a two-parameter Hill (log-logistic) model, as below:

$$V(\%) = 100/(1 + (D/IC_{50})^h) \tag{5}$$

where V is the percentage of cellular metabolic viability, D is the EGCG concentration, IC_{50} is the half-maximal inhibitory concentration, and h is the Hill slope. Parameters were estimated by weighted nonlinear least-squares fitting, using the standard deviations of the three technical replicates at each delivered EGCG dose as weights.[25]

Results and Discussion

Structural Characterization

The FE-SEM images of the nanoparticles are presented in Figure 2. The uncoated PLGA-EGCG nanoparticles exhibited an average diameter of 117 ± 8 nm, with spherical and uniform morphology and smooth surfaces. Other studies have

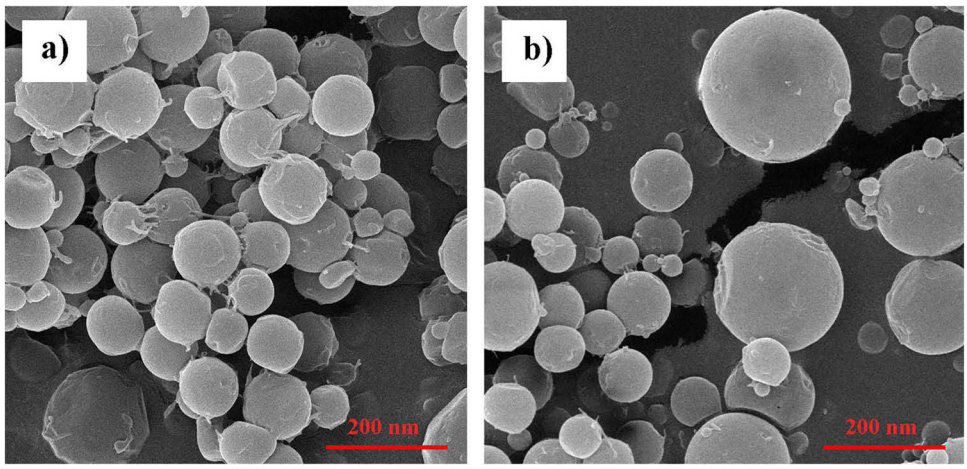


Figure 2 FE-SEM images of the uncoated PLGA-EGCG (**a**) and chitosan-coated (**b**) particulate samples.

https://doi.org/10.2147/IJN.S647028

employed the emulsion solvent evaporation method for the fabrication of nano/microparticles, reporting particle sizes ranging from 10 nm to 100 μm,[26,27] with parameters such as concentration, phase ratio, and stirring conditions can influence particle size. In contrast, the chitosan-coated PLGA nanoparticles showed an average diameter of 144 ± 6 nm with relatively smooth surfaces. Both powder samples exhibited slight surface adhesion, originating from particle bridging rather than particle agglomeration, due to the mechanical surface attachment of nanoparticles during the centrifugation process.[28] The thickness of the chitosan layer was estimated from the difference between the two mean diameters. Since the shell is added on both sides of the particle, the thickness is one half of the diameter increment: 13.5 ± 5.0 nm, with the uncertainty being propagated in quadrature. The FE-SEM images also revealed the presence of some surface pores on larger particles, which formed during solvent evaporation. Larger particles possess a lower surface-to-volume ratio and slower solvent evaporation rate; consequently, they require longer evaporation times and undergo more pronounced deformation, resulting in increased surface porosity.[29]

Nanoparticles within the size range of 50–200 nm have been reported to be suitable for tumor accumulation and can provide sufficient contrast for in vivo tumor delineation.[30–32] Particle sizes above 50 nm also improve local stability and reduce undesirable dispersion throughout the body. It has been reported that nanoparticles with sizes between 50 and 200 nm were internalized and distributed within cancer cells after 2 h, whereas particles with diameters around 500 nm remained primarily around the cell periphery.[33] Kazi et al[12] developed EGCG-loaded PLGA nanoparticles for cancer treatment and reported an average particle size of 169 nm, which they considered suitable for tumor penetration and breast cancer therapy. The diameter of 144 ± 6 nm measured here therefore lies within the size range generally considered promising for tumor accumulation.

Figure 3 presents the FTIR spectra of the fabricated samples for the evaluation of their chemical composition. The FTIR spectrum of the EGCG-loaded and chitosan-coated PLGA nanoparticles was consistent with previously reported

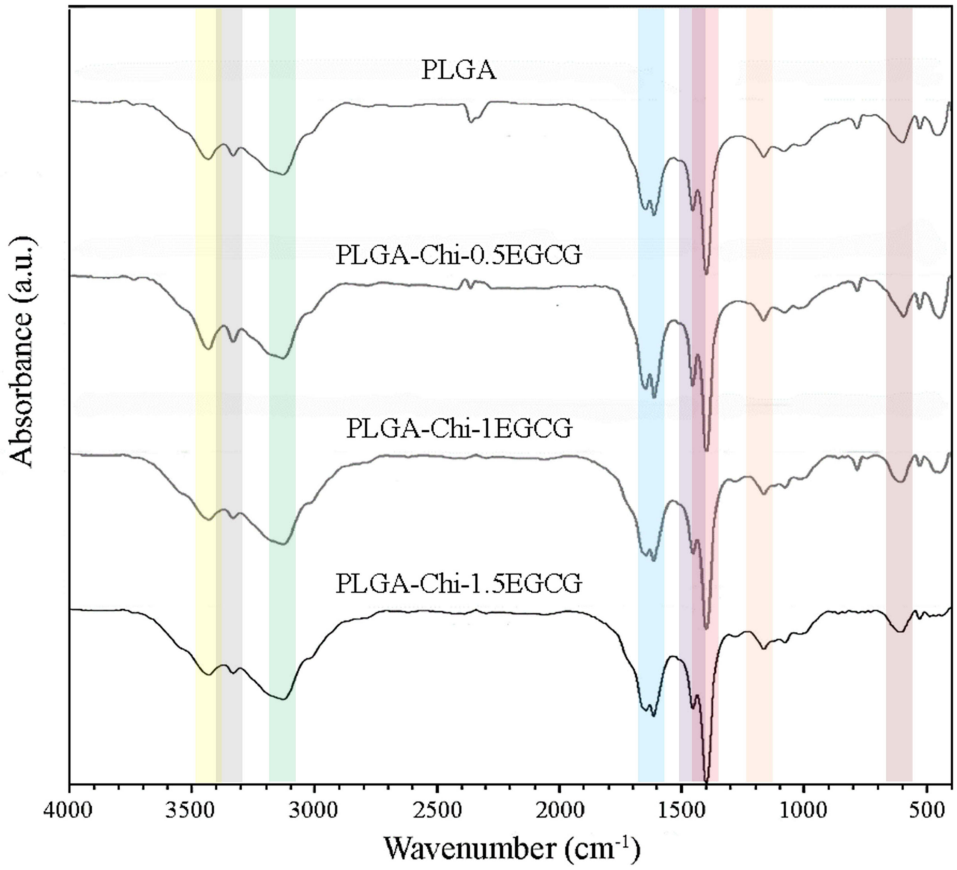


Figure 3 FTIR spectra of the fabricated nanoparticulate samples.

data. Characteristic PLGA bands included stretching vibrations at 3408 cm^{-1} corresponding to OH groups, 3170 cm^{-1} assigned to C–H stretching, and 1678 cm^{-1} corresponding to ester C=O stretching vibrations. The peak at 1249 cm^{-1} was assigned to C–CH_3 stretching vibrations, while the band at 1455 cm^{-1} corresponded to C–H stretching in methyl groups. The C–O stretching vibrations appeared at 1282 cm^{-1}.[34] In the FTIR spectrum of chitosan, the stretching vibrations of N–H and O–H groups were observed at 3336 cm^{-1}, while bending vibrations of primary and secondary amines appeared at 1649 cm^{-1} and 1610 cm^{-1}, respectively.[35] The FTIR spectrum of EGCG exhibited bands at 3491 cm^{-1} and 3381 cm^{-1} corresponding to OH groups attached to aromatic rings, strong bands at 1695 cm^{-1} and 1496 cm^{-1} corresponding to C=O groups, a strong band at 1410 cm^{-1} attributed to aromatic C–H groups of trihydroxy benzoate, and C–O stretching bands at 1272 cm^{-1} and 615 cm^{-1}.[36]

In conclusion, all characteristic peaks associated with EGCG, PLGA, and chitosan were detected in the FTIR spectra, confirming successful drug encapsulation within the PLGA nanoparticles and effective deposition of the chitosan coating on the nanoparticle surface. Moreover, the increased intensity of characteristic peaks at 3381 and 1410 cm^{-1} with increasing EGCG loading indicated the increased incorporation of EGCG into the nanoparticles. The FTIR spectra further demonstrated that most characteristic bands of EGCG, PLGA, and chitosan remained physically mixed with only minor peak shifts, indicating the absence of significant chemical reactions between EGCG and the carrier materials.

Drug Release Analysis

The drug release profiles of the nanoparticles in PBS are presented in Figure 4. The profiles exhibited a triphasic release pattern, initiated by a limited initial burst release attributed to drug accumulation on the particle surface. This stage was followed by a lag phase and subsequently by sustained and gradual release. The initial burst release during the first 24 h for the PLGA-EGCG, PLGA-Chi-0.5EGCG, PLGA-Chi-1EGCG, and PLGA-Chi-1.5EGCG samples was 25.7, 10.3, 12.6, and 15.6%, respectively. For the chitosan-coated samples, the release curves reached a plateau at 99% of the quantified payload on day 27, whereas the uncoated PLGA-EGCG sample reached its plateau on day 25. The encapsulation efficiencies for the PLGA-EGCG, PLGA-Chi-0.5EGCG, PLGA-Chi-1EGCG and PLGA-Chi-1.5EGCG samples were 88.7, 85.2, 88.8 and 86.5%, respectively, corresponding to drug loading contents of 0.89, 0.43, 0.89 and 1.30 wt%. At the nanoparticle concentration of 1 mg mL^{-1} used in the cell experiments, these correspond to EGCG doses of 8.87, 4.26, 8.88 and 12.98 µg mL^{-1}. Indeed, the PLGA-EGCG nanoparticles exhibited significantly higher initial burst release and overall release rate, which is considered undesirable for cancer therapy.[37,38] In contrast, the chitosan-coated PLGA nanoparticles demonstrated reduced burst release and slower EGCG release kinetics due to the presence of the chitosan coating.

The burst-release values of the coated formulations increase with the drug content. Given that burst release is generally attributed to drug situated at or close to the carrier surface, it is inferred that at low loading the drug is accommodated predominantly within the interior of the PLGA core. As the loading increases, the interior capacity approaches saturation, and a larger proportion of the drug partitions to the core surface and to the outermost region of the matrix, where the chitosan shell constitutes the only remaining barrier. The same mechanism accounts for the modest decrease in encapsulation efficiency at the highest loading (86.5% at 1.5 wt% against 88.8% at 1 wt%), since near-surface drug is also the fraction most readily lost during washing and centrifugation.

In order to characterize the release mechanism quantitatively, the cumulative profiles of all four formulations were fitted to the zero-order, first-order, Higuchi and Korsmeyer-Peppas models, with the fitted constants and coefficients of determination listed in Table 2. Over the complete profile, the Higuchi model provides the best description of the coated formulations. The Korsmeyer-Peppas release exponent is 0.46 for the uncoated PLGA-EGCG particles, consistent with Fickian diffusion from a spherical matrix, and 0.55–0.63 for the three chitosan-coated formulations, placing them in an anomalous, non-Fickian regime. That is, the chitosan shell does not merely slow an otherwise unchanged process: it shifts the transport mechanism from purely diffusion-controlled release out of the PLGA core to a coupled regime in which diffusion through the shell operates together with shell hydration and relaxation and with progressive erosion of the core. Considered over the sustained phase alone, the coated formulations are well described by a constant release rate: k_0 = 3.09, 2.79 and 2.64% per day with R^2 = 0.994, 0.978 and 0.968 for PLGA-Chi-0.5EGCG, PLGA-Chi-1EGCG and PLGA-Chi-1.5EGCG respectively, against R^2 = 0.919 for the uncoated reference. The coated formulations thus approach linear release during the sustained phase, although the profile taken as a whole is not of zero order.

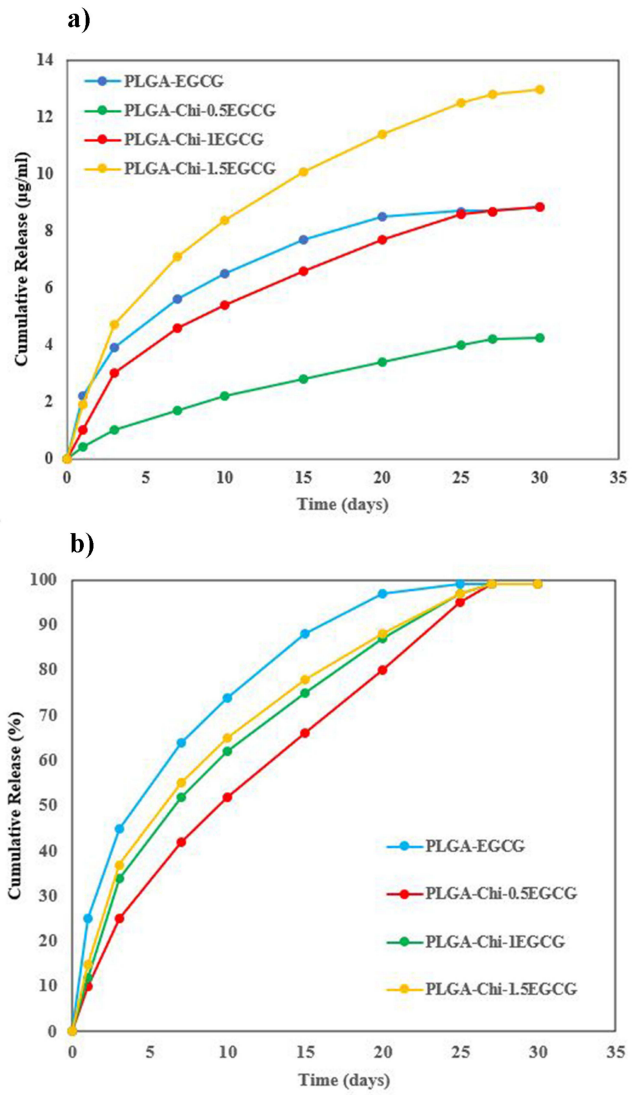


Figure 4 Cumulative EGCG released into the medium, expressed as concentration (**a**) and as percentage of the quantified payload (**b**).

According to the literature, an optimal release profile should generally include a controlled initial release phase to rapidly achieve therapeutic concentration, followed by prolonged sustained release within the minimum effective concentration range.[39] Zhao et al[40] developed PLGA-based nanocarriers loaded with the anticancer drug of doxorubicin and reported that an appropriate release profile for cancer therapy consists of an initial burst release below 20% followed by sustained release up to 30 days. Zhang et al[39] fabricated EGCG-loaded PLGA nanoparticles and reported 86% drug loading efficiency as satisfactory while also identifying sustained release up to 30 days as favorable for anticancer

Table 2 Kinetic Model Fitting of the Cumulative EGCG Release Profiles

Sample	Zero-Order k_0 (% d^{-1})/R^2	First-Order k_1 (d^{-1})/R^2	Higuchi k_h (% $d^{-0.5}$)/R^2	Korsmeyer–Peppas n/R^2
PLGA-EGCG	4.20/0.078	0.160/0.963	20.57/0.895	0.46/0.998
PLGA-Chi-0.5EGCG	3.79/0.889	0.085/0.968	17.95/0.974	0.63/0.997
PLGA-Chi-1EGCG	3.97/0.694	0.107/0.982	19.05/0.990	0.60/0.984
PLGA-Chi-1.5EGCG	4.01/0.581	0.116/0.980	19.35/0.985	0.55/0.987

activity. Several other studies have similarly reported that an initial burst release below 15% followed by continuous release for approximately 30 days represents a favorable release pattern for various anticancer agents.[41,42] Accordingly, the chitosan-coated formulations developed here fall within the ranges that these authors have reported as favorable.

Cellular Metabolic Viability

The MTT assay results for hepatic HepaRG cells are presented in Figure 5a. None of the formulations showed a significant reduction in the metabolic activity of HepaRG cells under the conditions tested, up to 5 days of exposure at 1 mg mL^{-1} nanoparticles corresponding to EGCG doses of up to 12.98 μg mL^{-1}. These findings are consistent with previous reports describing the relatively low cytotoxicity of EGCG toward non-tumorigenic hepatic cells at controlled

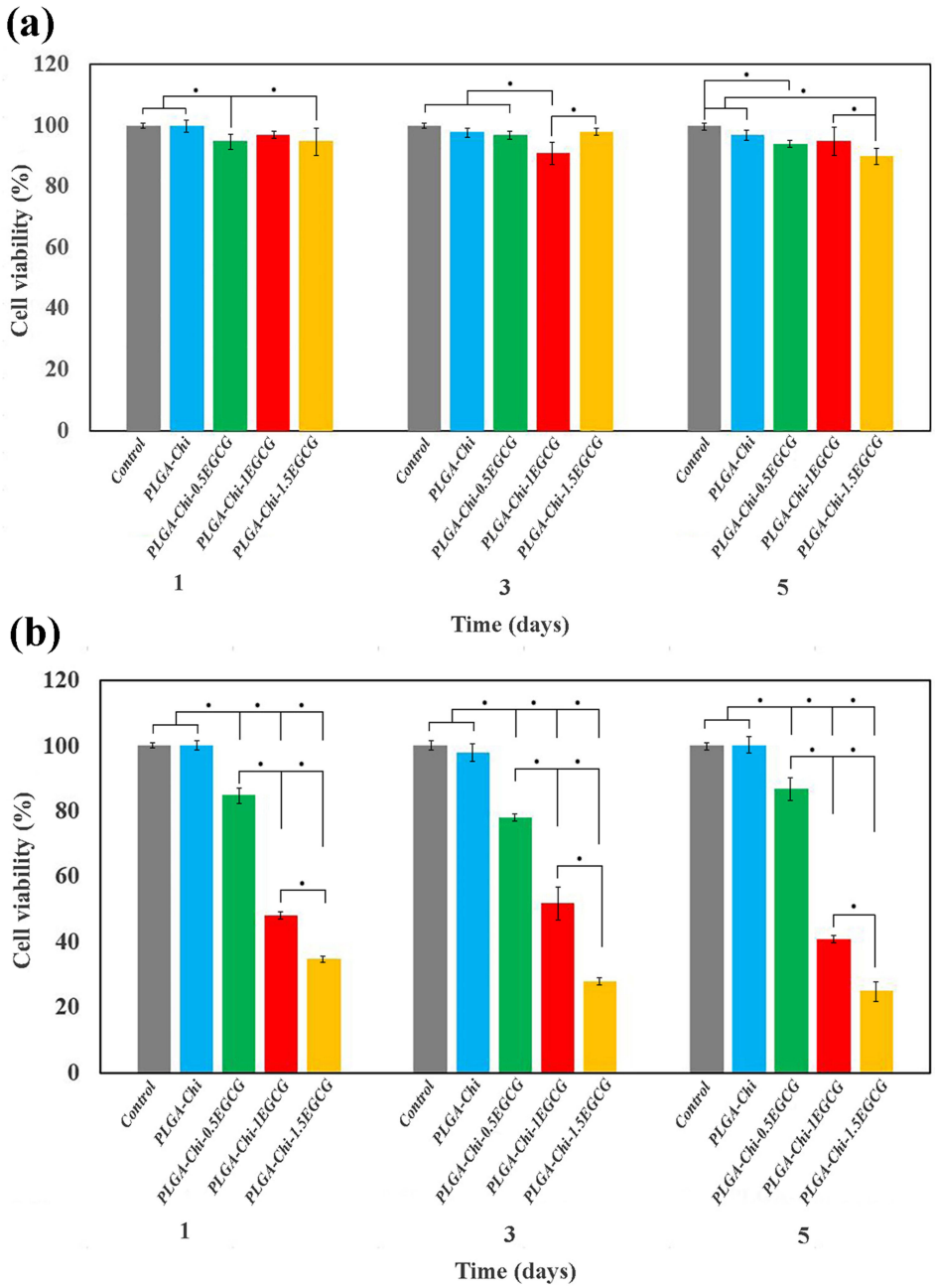


Figure 5 MTT metabolic-viability results for non-tumorigenic hepatic HepaRG cells (**a**) and HepG2 liver carcinoma cells (**b**), expressed as percentage of the untreated control, with *denoting statistically significant differences with $p < 0.05$.

https://doi.org/10.2147/IJN.S647028

concentrations. In these studies, the response of healthy cells to EGCG has been associated with mechanisms including antioxidant and anti-inflammatory effects, modulation of cellular signaling pathways, and regulation of proteins involved in cell survival and apoptosis.[43–45]

Metabolic viability on carcinoma HepG2 cells was also evaluated using the MTT assay (Figure 5b). The PLGA-Chi nanoparticles without EGCG did not reduce viability, whereas PLGA-Chi-0.5EGCG produced a small reduction and PLGA-Chi-1.5EGCG reduced viability to 35.1 ± 0.2% on day 1 and to 26.4 ± 1.8% on day 5, corresponding to 73.6% growth inhibition. All groups were tested at an equal nanoparticle mass concentration of 1 mg mL^{-1}, so that the EGCG concentration only varied across the groups and timepoints. The drug-free carrier acts as the zero-dose control, and its high viability in HepG2 and HepaRG cells indicates that the carrier itself does not measurably affect cellular metabolic activity under the conditions tested. Therefore, the response observed in the drug-loaded groups can be interpreted in relation to EGCG concentration.

The weighted Hill fit for HepG2 cells yielded an IC_{50} of 7.8 μg mL^{-1} (Hill slope, 2.5), compared with 8.2 μg mL^{-1} (Hill slope, 2.6) in the corresponding unweighted fit. For HepaRG cells, a valid IC_{50} was not reached because even at the highest dose tested (12.98 μg mL^{-1}), only 7.6% inhibition was measured, giving IC_{50} >13 μg mL^{-1} (outside the tested range). Accordingly, the differential response is presented as a model-free comparison at the matched dose: 73.6% inhibition in HepG2 versus 7.6% in HepaRG at 12.98 μg mL^{-1}, corresponding to a 9.7-fold difference in the measured response.

The time-dependent reduction in HepG2 metabolic viability is consistent with the release behavior described in Drug Release Analysis. The chitosan-coated formulations showed a limited initial burst followed by continued EGCG release, while the metabolic effect became more pronounced between days 1 and 5. This temporal concordance supports prolonged cellular exposure to EGCG as a plausible contributor to the sustained metabolic response. The observed reduction in HepG2 metabolic viability is also in line with the previously reported biological effects of EGCG in cancer cells. Previous studies have linked the activity of EGCG in cancer cells to modulation of apoptosis-related, inflammatory, and mitogenic signaling pathways.[43,46,47]

Comparing the measured metabolic activities with those reported in the literature, Kazi et al[12] developed folate-functionalized EGCG-loaded PLGA nanoparticles and reported approximately 48% cancer cell viability on day 1. Rocha et al[48] fabricated EGCG-loaded gum arabic–maltodextrin nanoparticles and observed approximately 60% cell viability on day 3. Narayanan et al[49] developed PLGA–casein core–shell nanoparticles loaded with paclitaxel and EGCG, reporting approximately 38% cell viability on day 3. The magnitude of the response observed here is within the range reported in these studies. However, the studies differ in cell line, exposure time, nanoparticle concentration, and delivered dose; therefore, these comparisons should be interpreted as contextual rather than quantitative.

Conclusions

Chitosan-coated PLGA nanoparticles loaded with EGCG were prepared by emulsion solvent evaporation and characterized with respect to morphology, composition, release kinetics, and in-vitro metabolic viability. The principal findings are as follows.

1. The particles were spherical with mean diameters of 117 ± 8 nm before coating and 144 ± 6 nm after coating, corresponding to an estimated dry chitosan shell thickness of 13.5 ± 5.0 nm. This size lies within the range generally reported as favorable for tumor accumulation, although no in-vivo evaluation was performed in this work.
2. Encapsulation efficiencies of 85.2–88.8% were achieved, corresponding to drug loading contents of 0.43–1.30 wt%.
3. The chitosan shell suppressed the 24 h burst release from 25.7% to 10.3–15.6% and extended the release period to a plateau from 25 to 27 days. Kinetic modelling showed that release from the coated formulations follows a Higuchi-type profile with Korsmeyer-Peppas exponents of 0.55–0.63, indicating anomalous, non-Fickian transport, against n = 0.46 and Fickian behavior for the uncoated reference. Over the sustained phase alone, the coated formulations approach a constant release rate of 2.6–3.1% per day.
4. The formulations reduced HepG2 metabolic viability in a concentration-dependent manner, to 26.4 ± 1.8% of the untreated control on day 5 (73.6% inhibition) for the highest loading, with a fitted IC_{50} of 8.2 μg mL^{-1}. Over the same dose range, HepaRG viability remained at or above 92.4%, above the 70% ISO 10993–5 threshold, and no IC_{50} was reached. The drug-free carrier was without effect in either line, so that the response is attributable to the delivered EGCG dose.

5. Although the present proof-of-concept study established the basic physicochemical characteristics of the nanoparticles, additional characterization of the chitosan coating, surface properties, and structural features would be valuable for further formulation optimization and development. A further limitation is that cell-free nanoparticle-plus-MTT controls were not included. Such controls are useful for determining whether the nanoparticles themselves interfere with the colorimetric assay through light scattering, absorbance, adsorption of formazan, or direct interaction with the tetrazolium reagent. Although the drug-free PLGA-Chi control showed no apparent reduction in MTT signal, this control does not exclude nanoparticle-related assay interference. Therefore, the viability results should be interpreted with this limitation in mind.

Acknowledgment

This research was supported by the Iran National Science Foundation (Grant No. 4014934).

Generative AI Disclosure

The authors also acknowledge the assistance of Claude-Opus 5.5 and ChatGPT GPT-6.1 Sol in improving the clarity and language quality of the manuscript. Following the use of these tools, the manuscript was carefully reviewed and revised by the authors, who assume full responsibility for the accuracy and integrity of the published content.

Disclosure

The authors report no conflict of interest in this work.

References

1. Zafar A, Khatoon S, Khan MJ, Abu J, Naeem A. Advancements and limitations in traditional anti-cancer therapies: a comprehensive review of surgery, chemotherapy, radiation therapy, and hormonal therapy. *Discov Oncol*. 2025;16:607. doi:10.1007/S12672-025-02198-8
2. AlQahtani AD, O'Connor D, Domling A, Goda SK. Strategies for the production of long-acting therapeutics and efficient drug delivery for cancer treatment. *Biomed Pharmacother*. 2019;113:108750. doi:10.1016/J.BIOPHA.2019.108750
3. Randisi F, Perletti G, Marras E, Gariboldi MB. Green tea components: in vitro and in vivo evidence for their anticancer potential in colon cancer. *Cancers*. 2025;17:623. doi:10.3390/CANCERS17040623
4. Liang G, Tang A, Lin X, et al. Green tea catechins augment the antitumor activity of doxorubicin in an in vivo mouse model for chemoresistant liver cancer. *Int J Oncol*. 2010;37:111–123. doi:10.3892/IJO_00000659/ABSTRACT
5. Tran PLCHB, Kim SA, Choi HS, Yoon JH, Ahn SG. Epigallocatechin-3-gallate suppresses the expression of HSP70 and HSP90 and exhibits anti-tumor activity in vitro and in vivo. *BMC Cancer*. 2010;10:276. doi:10.1186/1471-2407-10-276
6. Thangapazham RL, Singh AK, Sharma A, Warren J, Gaddipati JP, Maheshwari RK. Green tea polyphenols and its constituent epigallocatechin gallate inhibits proliferation of human breast cancer cells in vitro and in vivo. *Cancer Lett*. 2007;245:232–241. doi:10.1016/J.CANLET.2006.01.027
7. Fujiki H, Sueoka E, Watanabe T, Suganuma M. Synergistic enhancement of anticancer effects on numerous human cancer cell lines treated with the combination of EGCG, other green tea catechins, and anticancer compounds. *J Cancer Res Clin Oncol*. 2014;141:1511–1522. doi:10.1007/S00432-014-1899-5
8. Qutub M, Hussain UM, Tatode A, et al. Nano-Engineered Epigallocatechin Gallate (EGCG) delivery systems: overcoming bioavailability barriers to unlock clinical potential in cancer therapy. *AAPS Pharm Sci Tech*. 2025;26:137. doi:10.1208/S12249-025-03145-0
9. Sahadevan R, Singh S, Binoy A, Sadhukhan S. Chemico-biological aspects of (−)-epigallocatechin-3-gallate (EGCG) to improve its stability, bioavailability and membrane permeability: current status and future prospects. *Crit Rev Food Sci Nutr*. 2023;63:10382–10411. doi:10.1080/10408398.2022.2068500
10. Zhang S, Jiang W, Zhang Z, Zhu Y, Wang L, Fu J. A nanoparticle/oil double epigallocatechin gallate-loaded Pickering emulsion: stable and delivery characteristics. *LWT*. 2020;130:109369. doi:10.1016/J.LWT.2020.109369
11. Minnelli C, Stipa P, Sabbatini S, et al. Insights into PLGA-encapsulated epigallocatechin 3-gallate nanoparticles as a new potential biomedical system: a computational and experimental approach. *Eur Polym J*. 2023;182:111723. doi:10.1016/J.EURPOLYMJ.2022.111723
12. Kazi J, Sen R, Ganguly S, et al. Folate decorated epigallocatechin-3-gallate (EGCG) loaded PLGA nanoparticles; in-vitro and in-vivo targeting efficacy against MDA-MB-231 tumor xenograft. *Int J Pharm*. 2020;S0378–5173. doi:10.1016/j.ijpharm.2020.119449
13. Sanna V, Singh CK, Jashari R, et al. Targeted nanoparticles encapsulating (−)-epigallocatechin-3-gallate for prostate cancer prevention and therapy. *Sci Rep*. 2017;7:1–15. doi:10.1038/srep41573
14. Xu Y, Kim CS, Saylor DM, Koo D. Polymer degradation and drug delivery in PLGA-based drug–polymer applications: a review of experiments and theories. *J Biomed Mater Res Part B Appl Biomater*. 2017;105:1692–1716. doi:10.1002/JBM.B.33648
15. Kapoor DN, Bhatia A, Kaur R, Sharma R, Kaur G, Dhawan S. PLGA: a Unique Polymer for Drug Delivery, Ther. *Deliv*. 2015;6:41–58. doi:10.4155/TDE.14.91
16. Silva MM, Calado R, Marto J, Bettencourt A, Almeida AJ, Gonçalves LMD. Chitosan nanoparticles as a mucoadhesive drug delivery system for ocular administration, mar. *Drugs*. 2017;15:370. doi:10.3390/MD15120370
17. Chang PC, Tai WC, Luo HT, et al. Core-Shell poly-(D, L-Lactide-co-Glycolide)-chitosan nanospheres with simvastatin-doxycycline for periodontal and osseous repair. *Int J Biol Macromol*. 2020;158:627–635. doi:10.1016/j.ijbiomac.2020.04.183

18. Chronopoulou L, Massimi M, Giardi MF, et al. Chitosan-coated PLGA nanoparticles: a sustained drug release strategy for cell cultures. *Colloids Surf B Biointerfaces*. 2013;103:310–317. doi:10.1016/j.colsurfb.2012.10.063
19. Lee G, Ko YG, Bae KH, Kurisawa M, Kwon OK, Kwon OH. Green tea catechin-grafted silk fibroin hydrogels with reactive oxygen species scavenging activity for wound healing applications. *Biomater Res*. 2022;26:62. doi:10.1186/S40824-022-00304-3
20. Q2(R1) validation of analytical procedures: text and methodology guidance for industry. 2005. Available from: https://www.fda.gov/vaccines-blood-biologics/guidance-compliance-regulatory-information-biologics/biologics-guidances. Accessed September 12, 2026.
21. Peng X, Liu Z, Luo C, et al. PSMD12 promotes hepatocellular carcinoma progression by stabilizing CDK1. *Front Immunol*. 2025;16. doi:10.3389/FIMMU.2025.1581398
22. Andersson TB, Kanebratt KP, Kenna JG. The HepaRG cell line: a unique in vitro tool for understanding drug metabolism and toxicology in human. *Expert Opin Drug Metab Toxicol*. 2012;8:909–920. doi:10.1517/17425255.2012.685159
23. Monopoli MP, Åberg C, Salvati A, Dawson KA. Biomolecular coronas provide the biological identity of nanosized materials. *Nat Nanotechnol*. 2012;7:779–786. doi:10.1038/NNANO.2012.207
24. Bae MJ, Ishii T, Minoda K, et al. Albumin stabilizes (-)-epigallocatechin gallate in human serum: binding capacity and antioxidant property. *Mol Nutr Food Res*. 2009;53:709–715. doi:10.1002/MNFR.200800274
25. Ritz C, Baty F, Streibig JC, Gerhard D. Dose-response analysis using R. *PLoS One*. 2015;10:e0146021. doi:10.1371/JOURNAL.PONE.0146021
26. Astete CE, Sabliov CM. Synthesis and characterization of PLGA nanoparticles. *J Biomater Sci Polym Ed*. 2006;17:247–289. doi:10.1163/156856206775997322
27. Kizilbey K. Optimization of rutin-loaded PLGA nanoparticles synthesized by single-emulsion solvent evaporation method. *ACS Omega*. 2019;4:555–562. doi:10.1021/acsomega.8b02767
28. Qiao Z, Wang Z, Zhang C, Yuan S, Zhu Y, Wang J. PVAm–PIP/PS composite membrane with high performance for CO_2/N_2 separation. *AiChE J*. 2012;59:215–228. doi:10.1002/aic
29. Todaro B, Moscardini A, Luin S. Pioglitazone-loaded PLGA nanoparticles: towards the most reliable synthesis method. *Int J Mol Sci*. 2022;23:2522. doi:10.3390/ijms23052522
30. Awasthi R, Roseblade A, Hansbro PM, Rathbone MJ, Dua K, Bebawy M. Nanoparticles in cancer treatment: opportunities and obstacles. *Curr Drug Targets*. 2018;19:1696–1709. doi:10.2174/1389450119666180326122831
31. Aghebati-Maleki A, Dolati S, Ahmadi M, et al. Nanoparticles and cancer therapy: perspectives for application of nanoparticles in the treatment of cancers. *J Cell Physiol*. 2020;235:1962–1972. doi:10.1002/JCP.29126
32. Liang Q, Zeng J, Jiang Z, et al. MultivoidMagnetic nanoparticles as high-performancemagnetic particle imaging tracers for precise glioma detection. *Bioconjug Chem*. 2026;37:118–127. doi:10.1021/ACS.BIOCONJCHEM.5C00527
33. Haley B, Frenkel E. Nanoparticles for drug delivery in cancer treatment, Urol. *Oncol Semin Orig Investig*. 2008;26:57–64. doi:10.1016/J.UROLONC.2007.03.015
34. Wu J, Kong T, Yeung KWK, et al. Fabrication and characterization of monodisperse PLGA-alginate core-shell microspheres with monodisperse size and homogeneous shells for controlled drug release. *Acta Biomater*. 2013;9:7410–7419. doi:10.1016/j.actbio.2013.03.022
35. Xu F, Zhang J, Wang H, Jiang L. Facile fabrication of catechin-loaded PLGA/chitosan nanofibers for effective nursing care of wound-infecting bacterial pathogens and healing. *J Mater Res*. 2025;40:1574–1588. doi:10.1557/s43578-025-01595-7
36. Sindhuri GV, Mariappan G. Formulation and evaluation of epigallocatechin gallate and berberine- loaded chitosan nanoparticles. *Int J App Pharm*. 2023;15:178–89. doi:10.22159/ijap.2023v15i3.47410
37. Bhattacharjee S. Understanding the burst release phenomenon: toward designing effective nanoparticulate drug-delivery systems. *Ther Deliv*. 2021;12:21–36. doi:10.4155/TDE-2020-0099
38. Bai X, Smith ZL, Wang Y, Butterworth S, Tirella A. Sustained drug release from smart nanoparticles in cancer therapy: a comprehensive review. *Micromachines*. 2022;13:1623. doi:10.3390/MI13101623
39. Zhang L, Chen W, Tu G, et al. Enhanced chemotherapeutic efficacy of plga-encapsulated epigallocatechin gallate (EGCG) against human lung cancer. *Int J Nanomed*. 2020;15:4417–4429. doi:10.2147/IJN.S243657
40. Zhao J, Yang H, Li J, Wang Y, Wang X. Fabrication of pH-responsive PLGA(UCNPs/DOX) nanocapsules with upconversion luminescence for drug delivery. *Sci Rep*. 2017;7:1–11. doi:10.1038/S41598-017-16948-4
41. Ma G, Zhang C, Zhang L, et al. Doxorubicin-loaded micelles based on multiarm star-shaped PLGA–PEG block copolymers: influence of arm numbers on drug delivery. *J Mater Sci Mater Med*. 2016;27:1–15. doi:10.1007/S10856-015-5610-4/FIGURES/10
42. Cardoso MM, Peça IN, Bicho A. Impact of PEG content on doxorubicin release from PLGA-co-PEG nanoparticles. *Mater*. 2024;17:3544. doi:10.3390/MA17143544
43. Gan RY, Li HB, Sui ZQ, Corke H. Absorption, metabolism, anti-cancer effect and molecular targets of epigallocatechin gallate (EGCG): an updated review. *Crit Rev Food Sci Nutr*. 2018;58:924–941. doi:10.1080/10408398.2016.1231168
44. Granja A, Frias I, Neves AR, Pinheiro M, Reis S. Therapeutic potential of epigallocatechin gallate nanodelivery systems. *BioMed Res Int*. 2017;2017:5813793. doi:10.1155/2017/5813793
45. Singh BN, Shankar S, Srivastava RK. Green tea catechin, epigallocatechin-3-gallate (EGCG): mechanisms, perspectives and clinical applications. *Biochem Pharmacol*. 2011;82:1807–1821. doi:10.1016/J.BCP.2011.07.093
46. Rodponthukwaji K, Pingrajai P, Jantana S, et al. Epigallocatechin gallate potentiates the anticancer effect of AFP-siRNA-Loaded polymeric nanoparticles on hepatocellular carcinoma cells. *Nanomater*. 2023;14:47. doi:10.3390/NANO14010047
47. Cunha L, Coelho SC, Pereira MDC, Coelho MAN. Nanocarriers based on gold nanoparticles for epigallocatechin gallate delivery in cancer cells. *Pharmaceutics*. 2022;14:491. doi:10.3390/PHARMACEUTICS14030491/S1
48. Rocha S, Generalov R, Pereira MDC, Peres I, Juzenas P, Coelho MAN. Epigallocatechin gallate-loaded polysaccharide nanoparticles for prostate cancer chemoprevention. *Nanomedicine*. 2011;6:79–87. doi:10.2217/NNM.10.101
49. Narayanan S, Mony U, Vijaykumar DK, Koyakutty M, Paul-Prasanth B, Menon D. Sequential release of epigallocatechin gallate and paclitaxel from PLGA-casein core/shell nanoparticles sensitizes drug-resistant breast cancer cells. *Nanomedicine Nanotechnology Biol Med*. 2015;11:1399–1406. doi:10.1016/j.nano.2015.03.015

International Journal of Nanomedicine

Dovepress
Taylor & Francis Group

Publish your work in this journal

The International Journal of Nanomedicine is an international, peer-reviewed journal focusing on the application of nanotechnology in diagnostics, therapeutics, and drug delivery systems throughout the biomedical field. This journal is indexed on PubMed Central, MedLine, CAS, SciSearch®, Current Contents®/Clinical Medicine, Journal Citation Reports/Science Edition, EMBase, Scopus and the Elsevier Bibliographic databases. The manuscript management system is completely online and includes a very quick and fair peer-review system, which is all easy to use. Visit http://www.dovepress.com/testimonials.php to read real quotes from published authors.

Submit your manuscript here: https://www.dovepress.com/international-journal-of-nanomedicine-journal